AIP | Review of Scientific Instruments

Note: An asymmetric flexure mechanism for comb-drive actuators

M. Olfatnia, S. Sood, and S. Awtar

Citation: Rev. Sci. Instrum. **83**, 116105 (2012); doi: 10.1063/1.4767242
View online: http://dx.doi.org/10.1063/1.4767242
View Table of Contents: http://rsi.aip.org/resource/1/RSINAK/v83/i11
Published by the American Institute of Physics.

Additional information on Rev. Sci. Instrum.

Note: An asymmetric flexure mechanism for comb-drive actuators

M. Olfatnia, S. Sood, and S. Awtar
Department of Mechanical Engineering, University of Michigan, Ann Arbor, Michigan 48109, USA

(Received 12 September 2012; accepted 28 October 2012; published online 27 November 2012)

This Note presents a new asymmetric flexure design, the double parallelogram–tilted-beam double parallelogram (DP-TDP) flexure, that enables two times higher stroke in electrostatic comb-drive actuators, compared to the traditional symmetrically paired double parallelogram (DP-DP) flexure, while maintaining the same device footprint. Because of its unique kinematic configuration, the DP-TDP flexure provides an improved stiffness ratio between the bearing and actuation directions, thus delaying the on-set of sideways instability. Experimental testing of micro-fabricated comb-drive actuators with flexure beam length 1 mm and comb gap 5 μm demonstrates a stroke of 149 μm (at 86 V) for the proposed DP-TDP flexure, in comparison to 75 μm (at 45 V) for the traditional DP-DP flexure. © *2012 American Institute of Physics*. [http://dx.doi.org/10.1063/1.4767242]

Large actuation stroke ($>$100 μm) along with small device footprint and actuation effort is desirable in a wide range of MEMS applications.[1] One of the most common MEMS actuators is the electrostatic comb-drive actuator, given its simple design, fabrication, and operation.[1–3] A typical in-plane comb-drive actuator comprises a static comb and a moving comb, each with multiple fingers (N). When a voltage (V) is applied between these two combs, the moving comb displaces in the actuation direction (**Y**) with respect to the static comb, guided by a flexure mechanism. Ideally, the flexure mechanism provides low stiffness in this actuation direction and large stiffness in the bearing directions (**X** and **Θ**). When the negative stiffness associated with the electrostatic force between the two combs exceeds the flexure's positive stiffness in these bearing directions, the moving comb snaps sideways to the static comb. This snap-in instability is generally the primary factor limiting the actuator's stroke.[1,3]

To maximize the actuator's stroke while minimizing the actuation voltage and device footprint, the flexure mechanism should provide small stiffness in the actuation direction (K_y), along with large stiffness (K_x and K_θ) and minimal error motion (E_x and E_θ) in the bearing directions. The symmetrically paired double parallelogram (DP-DP) flexure, shown in Fig. 1, has been traditionally used in comb-drive actuators.[2,3] Even though K_y for this flexure is low, K_θ is high, and E_x and E_θ are zero for this flexure design, K_x drops sharply from a nominally high value at $Y = 0$ with increasing Y displacement.

Figure 2 plots the K_x/K_y stiffness ratio provided by the DP-DP and other flexures considered in this Note (obtained via finite elements analysis), along with the critical K_x/K_y stiffness ratio that is required to avoid snap-in in the **X** direction. The intersection of the flexure stiffness ratio and critical stiffness ratio curves corresponds to the snap-in condition and therefore the maximum actuation stroke. Due to the sharp drop in its K_x/K_y stiffness ratio, it is clear that the DP-DP flexure provides a small actuation stroke. For comb gap $G = 5$ μm, flexure beam length $L = 1000$ μm, and number of comb fingers $N = 70$, the measured stroke is 75 μm at 45 V.

This precipitous drop in bearing direction stiffness K_x is explained by the fact that the DP flexure geometry (Fig. 3(a)) represents a kinematically under-constrained design. When its motion stage is held fixed at a non-zero Y displacement, its secondary stage moves by $Y/2$ but remains kinematically free in the **Y** direction. Therefore, when an **X** direction force is applied on the motion stage, the nonlinear load-stiffening and softening effects in the flexure's constituent beams cause the secondary stage to move additionally from its nominal $Y/2$ displacement.[4] This additional **Y** direction displacement of the secondary stage leads to a disparity between the geometric contraction of the constituent beams along their length, thus producing an additional displacement at the motion stage and therefore an additional compliance in the **X** direction. In the DP-DP flexure (Fig. 1), this additional compliance and associated drop in K_x with increasing Y displacement happens in both the constituent DPs, resulting in the K_x/K_y stiffness ratio profile seen in Fig. 2.

DP and DP-DP flexures with pre-bent[1] or pre-tilted beams[5] have been used to shift the peak of the flexure's K_x/K_y stiffness ratio profile to larger values of Y displacement, where the required or critical K_x/K_y ratio is high. However, the sharp drop in the K_x/K_y stifness ratio remains unaffected. This leads to improvements in the comb-drive actuator stroke, but at the expense of stability robustness and bi-directional actuation capability. Separately, a tilted-beam double parallelogram (TDP) flexure design and its symmetrically paired version (TDP-TDP) have been reported.[6] While this design offers an improved nominal K_x stiffness (at $Y = 0$) in cases where the secondary stage lacks adequate structural rigidity, this design also exhibits the same precipitous drop in K_x stiffness, and therefore K_x/K_y stiffness ratio, as seen in the previous designs. The reason being that in all of these cases the secondary stage is kinematically under-constrained.

Here, we report a new asymmetric double parallelogram–tilted-beam double parallelogram (DP-TDP) flexure (Fig. 3) that employs a non-intuitive geometric arrangement to kinematically constrain the secondary stage of the TDP. This results in a significantly more gradual drop in the bearing stiffness K_x with increasing Y displacement, without affecting the K_y stiffness, thus leading to almost twice the stroke in comb-drive actuators as compared to the DP-DP flexure, but with the

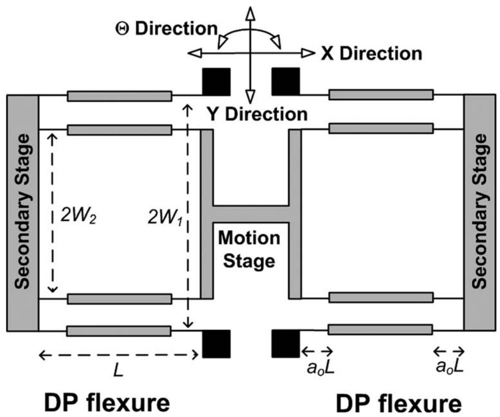

FIG. 1. Traditional DP-DP flexure.

same footprint, number of comb teeth, and effective moving mass.

The geometry of the TDP module within the DP-TDP flexure ensures that when the Y and Θ displacements of the motion stage are specified, there are two conflicting instantaneous centers of rotation (C_1 and C_2) created for the secondary stage (Fig. 3(b)). However, for this to happen, the $\mathbf{\Theta}$ rotation of the motion stage has to be specified, ideally to zero. This is not the case for a TDP by itself, which exhibits finite $\mathbf{\Theta}$ rotation. Therefore, to constrain this $\mathbf{\Theta}$ rotation to approximately zero, we employ a DP flexure (Fig. 3(a)). Thus, when the TDP flexure is coupled with the DP flexure (Fig. 3(c)), the two flexure modules serve distinct but highly complementary roles. Even though not good with K_x stiffness, the DP flexure provides a high K_θ stiffness which constrains the rotation of the combined motion stage. This rotational constraint, in turn, ensures that the secondary stage of the TDP is kinematically constrained such that its Y displacement remains approximately half that of the motion stage. This provides the desired improvement in the K_x stiffness behavior of the overall DP-TDP flexure. Moreover, with suitable choice of angles α and β, the overall K_y stiffness can be maintained at the same level as the DP-DP flexure. This results in better K_x/K_y versus Y characteristics, compared to the DP-DP flexure, as seen in Fig. 2. Furthermore, unlike the DP-DP flexure, the drop in the K_x/K_y stiffness ratio in this case is dictated by the weak elastokinematic effect, which can be further reduced via beam shape optimization (parameter a_0).[4] This enables even greater increase in the comb-drive actuation stroke, also shown in Fig. 2.

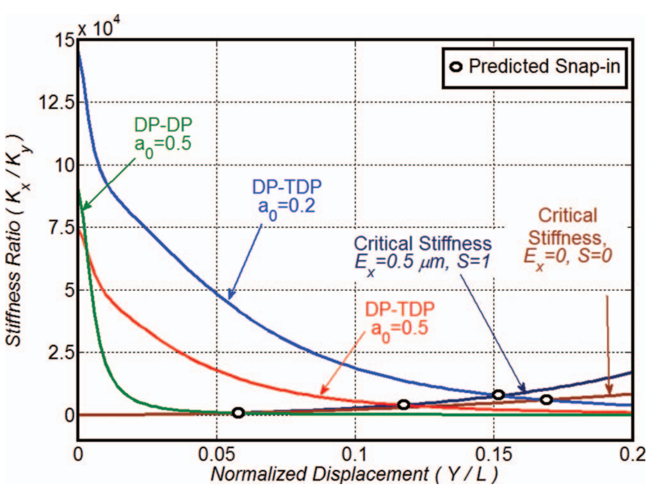

FIG. 2. (K_x/K_y) stiffness ratio for the DP-DP and DP-TDP flexures obtained via finite elements analysis. Critical (K_x/K_y) stiffness ratio curves for $G = 5\ \mu$m and $E_x = 0$ and $0.5\ \mu$m.

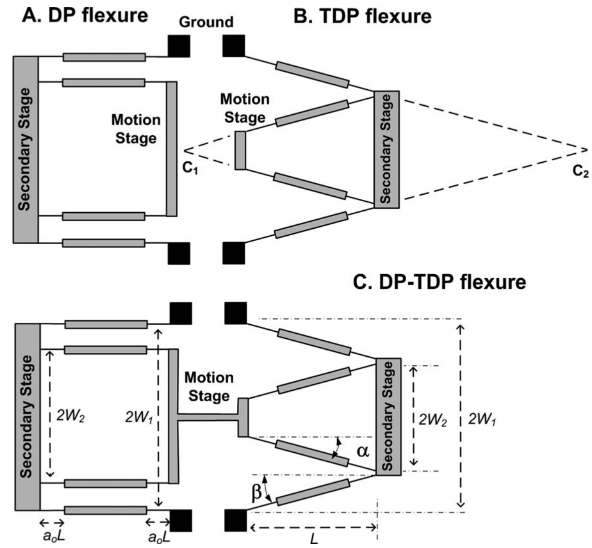

FIG. 3. Proposed DP-TDP flexure.

There exists at least one other design[7,8] that also restricts the sharp drop in K_x stiffness with increasing Y by kinematically constraining the $\mathbf{Y}$ direction displacement of the secondary stage to be half that of the motion stage by means of an external lever arm. However, this leads to a slightly higher K_y stiffness, larger device footprint, as well as a higher effective moving mass. In the asymmetric DP-TDP flexure, the secondary stage of the TDP is kinematically constrained without any additional topological features, thus retaining the same footprint, moving mass, and K_y stiffness as the baseline DP-DP flexure.

The primary goal of this Note is to demonstrate a larger comb-drive actuation stroke via the DP-TDP flexure, in comparison to the DP-DP flexure, while minimizing device footprint and actuation voltage. Therefore, as the first step in this design and validation process, the DP-DP flexure dimensions are chosen to provide low K_y and high K_θ over a large Y displacement range and high K_x at $Y = 0$. The resulting flexure and comb-drive dimensions are compiled in Table I. To design the DP-TDP flexure, the only dimensions that remain to be selected are the tilt angles α and β in its TDP module. For this purpose, nonlinear finite elements analysis (FEA) was performed to determine the stiffness and error motions of the DP-TDP flexure at different values of Y displacement over a practical range of α and β (± 0.25 rad). This analysis showed that the expected improvement in K_x occurs when either α or β, or both are greater than 0.1 rad. A low value of K_y, equal to that of the DP-DP flexure, is maintained as long as both α and β are greater than 0.1 rad. Error motion E_x is minimized when α and β are approximately equal. Furthermore, for the dimensions considered, K_θ was large enough to be ignored in comparison to K_x, and E_θ was small enough to be ignored in comparison to E_x. This leads to considerable simplification

TABLE I. Fabricated devices. Comb-drive dimensions are same in all cases: $G = 5$ μm, comb-finger length $L_f = 190$ μm, in-plane thickness $T_f = 6$ μm, out-of-plane thickness $H_f = 50$ μm, and $N = 70$. Flexure beam length $L = 1000$ μm and in-plane thickness $T = 3$ μm in all cases. All dimensions are in micrometers (μm).

Flexure design	W_1	W_2	a_0	Designed stroke $S = 0$	Designed stroke $S = 1$	Measured stroke	Voltage (V)
DP-DP	525	325	0.5	76.7	54.2	75	45
DP-TDP	525	325	0.5	141	122	125	70
DP-TDP	525	325	0.2	178	156	149	86

in the stability and actuation conditions,[1,3] which are stated below:

$$\frac{K_x}{K_y} = \frac{2Y_{\max}^2}{G^2}\left[1 + S(E_x)\right], \tag{1}$$

$$K_y \cdot Y = \frac{\varepsilon_0 H_f}{G} N V^2. \tag{2}$$

The first equation above corresponds to snap-in in the **X** direction at $Y = Y_{\max}$ and assumes negligible initial finger engagement. Here, S is a positive margin of stability to account for the increase in required K_x/K_y stiffness ratio when an error motion E_x due to the flexure kinematics or manufacturing imperfections is present. In Eq. (2), ε_0 is dielectric constant of air and H_f is out-of-plane thickness of the comb fingers. At the maximum actuation stroke, $Y = Y_{\max}$, the above two equations may be simultaneously solved to obtain:

$$\frac{Y_{\max}^2}{NV^2} = \varepsilon_0 H_f \left[\sqrt{\frac{K_x}{2K_y^3\left(1 + S(E_x)\right)}}\right]_{@Y=Y_{\max}}. \tag{3}$$

Thus, to maximize the actuation stroke ($Y_{\max}$) while minimizing the actuation voltage (V) and device footprint (N), it is clear that one has to maximize the right hand side of the above equation at the desired $Y_{\max}$. This objective function along with the above FEA results were then used to select $\alpha = 0.11$ rad and $\beta = 0.14$ rad. Once the optimal values of α and β were chosen, the comb gap G and beam shape parameter a_0 were selected to maximize the actuation stroke for an allowable NV^2. The final dimensions of the resulting DP-TDP flexures and associated comb-drives are summarized in Table I.

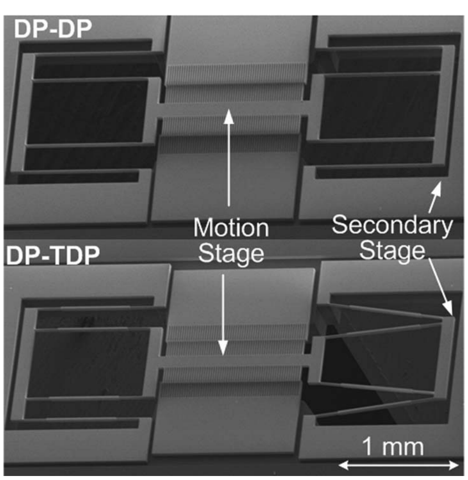

FIG. 4. SEM image of micro-fabricated comb-drive actuators based on the DP-DP and DP-TDP flexures.

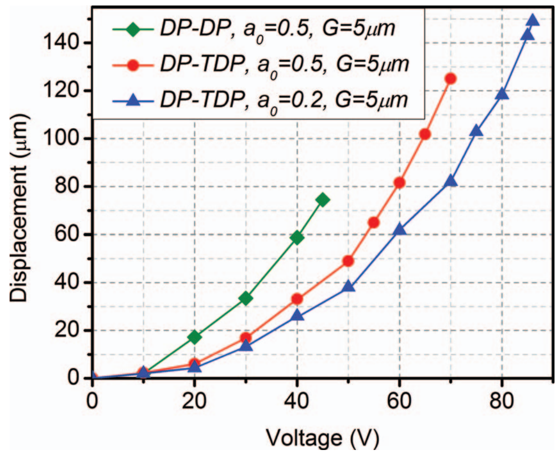

FIG. 5. Displacement measurements for comb-drive actuators based on the DP-DP and DP-TDP flexures.

Comb-drive actuators based on the above DP-DP and DP-TDP flexures were micro-fabricated with silicon on insulator wafers with a device layer of 50 μm (Fig. 4). The experimentally measured displacement versus voltage curves for these actuators are shown in Fig. 5. The measured actuation stroke at snap-in for the conventional DP-DP flexure with the above dimensions was 75 μm at 45 V. The actuation stroke for a DP-TDP flexure with the same dimensions was measured to be 125 μm at 70 V. As expected, an even higher stroke of 149 μm was measured for a DP-TDP flexure with the same overall dimensions but using reinforced beams ($a_0 = 0.2$). On comparison with the predicted actuation stroke (Table I), these experimental measurements also show that for the DP-DP flexure, where error motions (E_x) are absent, a stability margin of $S = 0$ is acceptable. However, for the DP-TDP, which exhibits finite error motions, maintaining a stability margin of $S = 1$ is necessary.

In summary, this Note presents a novel DP-TDP flexure design, shows its superior K_x stiffness performance via FEA, and experimentally demonstrates that it provides two times higher actuation stroke in an electrostatic comb-drive actuator, as compared to the traditional DP-DP flexure. This improvement in stroke is achieved while maintaining the same device footprint, moving mass, and fabrication process. The DP flexure and the TDP flexure, individually, do not provide good performance. Instead, based on kinematic design principles, we combine the two, making intentional use of asymmetry, which is generally counter-intuitive, to produce better overall performance.

[1] J. D. Grade, H. Jerman, and T. W. Kenny, J. Microelectromech. Syst. **12**(3), 335 (2003).
[2] W. C. Tang, T. C. H. Nguyen, and R. T. Howe, Sens. Actuators **20**(1–2), 25 (1989).
[3] R. Legtenberg, A. W. Groeneveld, and M. Elwenspoek, J. Micromech. Microeng. **6**(3), 320 (1996).
[4] S. Awtar, A. H. Slocum, and E. Sevincer, J. Mech. Des. **129**(6), 625 (2007).
[5] G. Y. Zhou and P. Dowd, J. Micromech. Microeng. **13**(2), 178 (2003).
[6] S. Kota, J. Hetrick, Z. Li, and L. Saggere, IEEE/ASME Trans. Mechatron. **4**(4), 396 (1999).
[7] R. V. Jones and I. R. Young, J. Sci. Instrum. **33**(1), 11 (1956).
[8] D. M. Brouwer, A. Otten, J. B. C. Engelen, B. Krijnen, and H. M. J. R. Soemers, in *Proceedings of the EUSPEN International Conference*, Delft, 2010.